

Perturbations of the Stratosphere and Mesosphere by Aerospace Vehicles

R. C. WHITTEN*

NASA Ames Research Center, Moffett Field, Calif.

AND

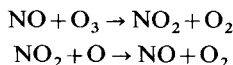
R. P. TURCO†

R and D Associates, Santa Monica, Calif.

The work discussed in this paper is directed toward possible environmental effects of high-altitude craft such as the SST and the space shuttle vehicle. The model includes the chemistry of the O-H-N system and vertical eddy transport. When the predicted NO_x emission from an SST fleet projected for 1990 is introduced, it is found that the reduction in ozone column density is less than 15%. Furthermore, flight altitudes near 16 km lead to ozone reductions which are much less than are associated with flight altitudes near 20 km. The effect of projected space shuttle operations on mesospheric composition is negligible.

Introduction

WE have developed a one-dimensional model, including eddy transport, of the minor constituents (the O-H-N-C-S system) in the upper atmosphere. The photochemistry involves about 100 reactions and about 30 species in the above-named family of compounds. In particular, the model treats the reactions of nitrogen oxides and water vapor derivatives with odd oxygen, one of the principal environmental concerns at present. Nitrogen oxides (NO_x) react catalytically with odd oxygen (i.e., O and O_3), changing the latter to O_2 via the reaction sequence



The model also includes provision for removing NO_x derivatives by transport through the lower boundary.

Nitrogen oxides occur in the atmosphere as a result of upward convection of N_2O from the surface of the Earth and production of atomic nitrogen at high altitudes by ionic reactions and by photodissociation of N_2 ; the nitrogen atoms react with O_2 to produce NO. The metastable species $\text{N}(^2\text{D})$ is much more effective in producing nitric oxide because the reaction $\text{N}(^2\text{D}) + \text{O}_2 \rightarrow \text{NO} + \text{O}$ has very small activation energy. To treat properly the chemistry that leads to NO production, one must use a model that extends upward to about 200 km and that includes the pertinent ion reactions. We avoid such complexity by using the results of Strobel,¹ which take the form of effective rates of production below 120 km and a downward flux of $\sim 10^8 \text{ cm}^2 \text{ sec}^{-1}$ at the upper boundary.

As a result of combustion processes, jet engines mounted in a fleet of supersonic transports will introduce copious quantities of NO at stratospheric altitudes. Space shuttle re-entry will also produce NO as a result of atmospheric heating, but at greater altitudes, 65–90 km. This paper will explore the effect of such perturbations on the ozone balance of the atmosphere.

Model

Our model of the distribution of minor constituents in the stratosphere and mesosphere includes both chemistry and

vertical transport. The mass continuity equation for each constituent is

$$\partial n_i / \partial t + \partial \Phi_i / \partial z = P_i - l_i n_i \quad (1)$$

where Φ_i is the particle flux in the vertical direction:

$$\Phi_i = v n_i - K_e \left[\partial n_i / \partial z + (1/H + 1/T) dT/dz n_i \right] - D_i \left[\partial n_i / \partial z + (1/H_i + dT/T dz) n_i \right] \quad (2)$$

Here, n_i is the concentration of the i th constituent; K_e and D_i are the eddy and molecular diffusion coefficients, respectively; H is the mean atmospheric scale height; H_i is the scale height of the i th constituent above the turbopause; T is the temperature; v is the convective velocity (neglected in this paper); and P_i and $l_i n_i$ are the production and loss rates per unit volume of the i th constituent. All the chemistry is represented in terms P_i and $l_i n_i$. Neglect of horizontal transport is a limitation of our model; the model is now being extended to two dimensions and results will be reported at a future date.

The eddy diffusion coefficient, which is altitude dependent, is a strictly phenomenological parameter chosen so that the flux tends to maintain each constituent at a constant mixing ratio. The concept of eddy mixing arises in the "mixing length" theory which fails to consider the fact that eddies of different scales have different effects. Nevertheless, the concept is useful because it does crudely approximate the behavior of trace gases in the upper atmosphere and because it is the simplest approach available. The K_e profiles (Fig. 1) bracket the range of possible

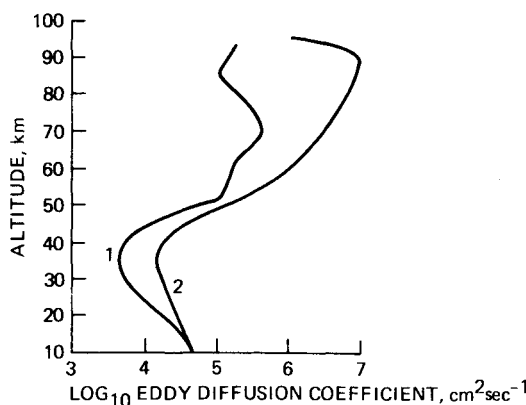


Fig. 1 Profiles of eddy diffusion coefficient; 1) Hays and Oliveiro,² and 2) S. P. Zimmerman.³

Presented as Paper 73-539 at the AIAA/AMS International Conference on the Environmental Impact of Aerospace Operations in the High Atmosphere, Denver, Colo., June 11–13, 1973; submitted October 9, 1973; revision received March 23, 1974.

Index category: Atmospheric, Space, and Oceanographic Sciences.

* Research Scientist, Space Science Division.

† Research Scientist.

Table 1 Chemical parameters: Reaction rate coefficients for the O-H-N system^a

Number	Process	Rate coefficient	Reference
1	$O + O_2 + M \rightarrow O_3 + M$	$1.1 \times 10^{-34} e^{507/T}$	4
2	$O + O + M \rightarrow O_2 + M$	$3 \times 10^{-33} (300/T)^3$	5
3	$O + O_3 \rightarrow O_2 + O_2$	$2 \times 10^{-11} e^{-2410/T}$	6
4	$O(^1D) + O_3 \rightarrow 2O_2$	2.5×10^{-10}	7
5	$O(^1D) + H_2O \rightarrow 2OH$	3×10^{-10}	^b
6	$O(^1D) + M \rightarrow O + M$	8×10^{-11}	8
7	$O + OH \rightarrow H + O_2$	3.8×10^{-11}	9
8	$O_3 + H \rightarrow OH + O_2$	$1.5 \times 10^{-12} T^{1/2}$	10
9	$O + HO_2 \rightarrow OH + O_2$	1×10^{-11}	11
10	$O_2 + OH \rightarrow HO_2 + O$	$3.8 \times 10^{-12} e^{-1250/T}$	12
11	$H + O_2 + M \rightarrow HO_2 + M$	$1.9 \times 10^{-32} e^{236/T}$	13
12	$NO + O_3 \rightarrow NO_2 + O_2$	$9 \times 10^{-13} e^{-1200/T}$	^b
13	$O + NO_2 \rightarrow NO + O_2$	9.1×10^{-12}	14
14	$NO + O + M \rightarrow NO_2 + M$	$1 \times 10^{-32} e^{930/T}$	15
15	$OH + OH \rightarrow H_2O + O$	$1 \times 10^{-11} e^{-550/T}$	9
16	$OH + HO_2 \rightarrow H_2O + O_2$	2×10^{-10}	16
17	$H + HO_2 \rightarrow 2OH$	$2.8 \times 10^{-10} e^{-1000/T}$	17
18	$H + HO_2 \rightarrow H_2 + O_2$	$3.2 \times 10^{-11} e^{-500/T}$	18
19	$H + HO_2 \rightarrow H_2O + O$	$1.6 \times 10^{-11} e^{-500/T}$	18
20	$HO_2 + HO_2 \rightarrow H_2O_2 + O_2$	$1.7 \times 10^{-11} e^{-500/T}$	^b
21	$H_2O_2 + OH \rightarrow H_2O + HO_2$	$1.7 \times 10^{-11} e^{-910/T}$	9
22	$H_2O_2 + O \rightarrow H_2O + O_2$	$1.5 \times 10^{-13} e^{-2000/T}$	19
23	$H_2O_2 + O \rightarrow OH + HO_2$	$1 \times 10^{-13} e^{-2000/T}$	19
24	$O(^1D) + H_2 \rightarrow OH + H$	1.9×10^{-10}	20
25	$O(^1D) + H_2O_2 \rightarrow H_2O + O_2$	1×10^{-10}	^c
26	$O_3 + HO_2 \rightarrow OH + 2O_2$	$2.7 \times 10^{-11} e^{-1750/T}$	^d
27	$OH + OH + M \rightarrow H_2O_2 + M$	3×10^{-30}	21
28	$N_2O + O(^1D) \rightarrow 2NO$	1.0×10^{-10}	20
29	$N_2O + O(^1D) \rightarrow N_2 + O_2$	8.0×10^{-11}	20, 22
30	$N + O_3 \rightarrow NO + O_2$	$3.4 \times 10^{-11} e^{-1200/T}$	^e
31	$N + NO \rightarrow O + N_2$	$2.6 \times 10^{-11} e^{-167/T}$	15
32	$N + O_2 \rightarrow NO + O$	$5 \times 10^{-13} T^{1/2} e^{-3650/T}$	23
33	$N + NO_2 \rightarrow N_2O + O$	8×10^{-12}	24
34	$N + NO_2 \rightarrow 2NO$	6×10^{-12}	24
35	$N + NO_2 \rightarrow N_2 + O_2$	4×10^{-12}	24
36	$NO_2 + O_3 \rightarrow NO_3 + O_2$	$1 \times 10^{-11} e^{-3500/T}$	^b
37	$NO_2 + O + M \rightarrow NO_3 + M$	$1.4 \times 10^{-23} / (1.3 \times 10^{-12} [M] + 5 \times 10^7)$	^f
38	$NO + NO_3 \rightarrow 2NO_2$	$5.7 \times 10^{-12} (300^\circ)$	25
39	$NO_2 + NO_3 + M \rightarrow N_2O_5 + M$	$1 \times 10^{-22} / (1.7 \times 10^{-10} [M] + 2 \times 10^8)$	^g
40	$N_2O_5 + M \rightarrow NO_2 + NO_3 + M$	$8.3 \times 10^{-8} e^{-8300/T}$	26
41	$NO + HO_2 \rightarrow NO_2 + OH$	$1.7 \times 10^{-11} e^{-1200/T}$	27
42	$NO_2 + H \rightarrow NO + OH$	$9.6 \times 10^{-10} e^{-900/T}$	^b
43	$NO_2 + OH + M \rightarrow HNO_3 + M$	$2.8 \times 10^{-22} / (4 \times 10^{-11} [M] + 4.8 T^3)$	^h
44	$HNO_3 + O \rightarrow OH + NO_3$	1×10^{-14}	^b
45	$HNO_3 + OH \rightarrow H_2O + NO_3$	$1.6 \times 10^{-12} e^{-1000/T}$	^b
46	$NO + OH + M \rightarrow HNO_2 + M$	$1.8 \times 10^{-32} e^{1135/T}$	28
47	$HNO_2 + O \rightarrow OH + NO_2$	1×10^{-14}	ⁱ
48	$HNO_2 + OH \rightarrow H_2O + NO_2$	$1.4 \times 10^{-12} e^{-1000/T}$	^b
49	$OH + H \rightarrow O + H_2$	$1.0 \times 10^{-11} e^{-3700/T}$	29
50	$NO_3 + O \rightarrow NO_2 + O_2$	$1 \times 10^{-12} e^{-1500/T}$	^j
51	$OH + O + M \rightarrow HO_2 + M$	1×10^{-31}	30
52	$H + H + M \rightarrow H_2 + M$	8.3×10^{-33}	9
53	$N + OH \rightarrow NO + H$	5.8×10^{-11}	21
54	$NO + HO_2 + M \rightarrow HNO_3 + M$	1×10^{-33}	^j
55	$O(^1D) + N_2 + M \rightarrow N_2O + M$	1×10^{-38}	^k

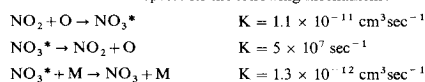
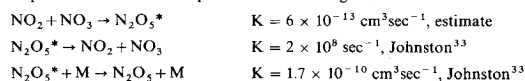
^a In units of $\text{cm}^6\text{sec}^{-1}$ for termolecular reactions, $\text{cm}^3\text{sec}^{-1}$ for bimolecular reactions, and sec^{-1} for unimolecular reactions.^b The value adopted here was suggested by the recent reviews of available rate constant data published by the National Bureau of Standards, R. F. Hampson, ed., National Bureau of Standards Repts. NBS-10692 and NBS-10828, 1972.^c Order-of-magnitude estimate suggested by other $O(^1D)$ reactions.^d Estimated value assumes a 300°K rate, $8 \times 10^{-14} \text{ cm}^3\text{sec}^{-1}$, and an activation energy of 3.5 kcal/mole.^e Value of Phillips and Schiff³¹ at 300°K and an activation energy of 2.4 kcal/mole.^f The equivalent pressure-dependent rate constant represents the following mechanism:The rate data are taken from Klein and Herron.³² NO_3^* is assumed to be in a steady state at all times. The low-pressure limit yields a rate constant $2.8 \times 10^{-31} \text{ cm}^6\text{sec}^{-1}$.^g The equivalent pressure-dependent rate constant represents the following mechanism:The low-pressure limit for this rate is then $5 \times 10^{-31} \text{ cm}^6\text{sec}^{-1}$.^h The equivalent pressure-dependent rate constant is formed using data obtained from Crutzen (private communication) and Anderson and Kaufman.¹² The low-pressure value of $6 \times 10^{-23} T^{-3} \text{ cm}^6\text{sec}^{-1}$ agrees well with the recent measurement of Westenberg and deHaas.²⁸ⁱ Assumed to be the same as the rate of $\text{HNO}_3 + \text{O}$.^j Adopted rate constant.^k Simonaitis et al.³⁴ show that $k < 7 \times 10^{-36} \text{ cm}^6\text{sec}^{-1}$. This reaction is marginal.

Table 2 Photodissociation rates for O-H-N system^a

Number	Process	Rate coefficient	Reference
J1	$O_2 + h\nu \xrightarrow{\lambda < 1759\text{\AA}} O(^1D) + O(^3P)$	2.1×10^{-6}	35-38
J2	$O_2 + h\nu \xrightarrow{1759 \leq \lambda < 2424\text{\AA}} 2O(^3P)$	3.8×10^{-8}	
J3	$O_3 + h\nu \xrightarrow{\lambda < 3100\text{\AA}} O_2(^1\Delta_g) + O(^1D)$	9.6×10^{-3}	
J4	$O_3 + h\nu \xrightarrow{3100 < \lambda < 6110\text{\AA}} O_2(^1\Delta_g) + O(^3P)$	4.1×10^{-4}	39-41
J5	$O_3 + h\nu \xrightarrow{\lambda \leq 11800\text{\AA}} O_2(^1\Sigma^-_g) + O(^3P)$	2.7×10^{-5}	
J6	$NO + h\nu \rightarrow N + O$	1.0×10^{-5}	^b
J7	$NO_2 + h\nu \rightarrow NO + O$	1.1×10^{-2}	42-44
J8	$NO_3 + h\nu \rightarrow NO + O_2$	1.1×10^{-3}	^c
J9	$N_2O + h\nu \rightarrow N_2 + O(^1D)$	2.4×10^{-6}	45-47
J10	$N_2O_5 + h\nu \rightarrow 2NO_2 + O$	1.2×10^{-4}	48
J11	$HNO_2 + h\nu \rightarrow OH + NO$	1.1×10^{-3}	^d
J12	$HNO_3 + h\nu \rightarrow OH + NO_2$	2×10^{-4}	49, 50 ^e
J13	$H_2O + h\nu \rightarrow OH + H$	7.1×10^{-6}	51
J14	$H_2O_2 + h\nu \rightarrow 2OH$	1.5×10^{-4}	52, 53
J15	$HO_2 + h\nu \rightarrow OH + O$	1.1×10^{-3}	16, 54

^a In units of sec^{-1} at zero optical depth.^b Extrapolated from data below 55 km provided by G. Brasseur (private communication, 1972). Data are consistent with that of Strobel.¹^c Assumed equal to 1/10 of rates of J7.^d Assumed equal to 1/10 of rate of J7.⁵⁵^e Johnston concluded that the quantum yield of J12 is very close to unity for his measurements. Hence, the process leading to $H + NO_3$ can be ignored. Solar flux from Detwiler et al.⁵⁶ and Parkinson and Reeves.⁵⁷

values reasonably well.^{2,3} We know that we can expect quite large values ($\approx 10^5$ – $10^6 \text{ cm}^2 \text{ sec}^{-1}$) in the mesosphere, because the atmosphere is relatively unstable against vertical motion there, while allowed values for K_e in the stratosphere must be much smaller, i.e., 10^3 to $10^4 \text{ cm}^2 \text{ sec}^{-1}$, because of the great stability of that region. Later, we shall present some results, using the two profiles of K_e shown in Fig. 1, and make some comparisons to determine the sensitivity of various minor constituents to variations in the eddy diffusion coefficients.

The chemical reactions and photodissociation processes, which are included in the model, are listed in Tables 1 and 2, respectively. A number of permitted reactions have been omitted because their contributions to the over-all reaction scheme have been found by calculation to be negligible. In some cases, it was necessary to estimate reaction rate coefficients and photolysis rates because they have not yet been measured. Such estimates are explained by notes in the tables. Where pertinent cross sections are known, photolysis rates have been computed by the usual relation

$$q_i(z) = n_i(z) \int \epsilon_{\lambda,i} Q_{\lambda,i} I_{\lambda} e^{-\tau_{\lambda}} d\lambda \quad (3)$$

$$\tau_{\lambda}(z) = \tau_{\lambda,O_3} + Q_{\lambda,O_2} \int_z^{\infty} n_{O_2}(z) dz \sec \chi \quad (4)$$

where $Q_{\lambda,i}$ is the photoabsorption cross section, $\epsilon_{\lambda,i}$ is the quantum yield, τ_{λ} is the optical depth (due to absorption by O_2 and O_3), I_{λ} is the solar photon flux per wavelength interval at the top of the atmosphere, and χ is the solar zenith angle. O_2 absorption in the Schumann-Runge bands has been treated more rigorously using a band absorption model. The results for this model are similar to the results of a detailed study of O_2 absorption by Hudson and Mahle.³⁵ During each computation the photodissociation rates were recomputed whenever the total vertical O_3 column changed by 1.5%.

The set of differential equations [Eqs. (1) and (2)] was transformed into the corresponding finite-difference set, using a semi-implicit method (i.e., implicit in the transport and loss terms, explicit in the production terms), and solved by a "marching" technique from 10–120 km altitude.⁵⁸

The implicit method for solving Eqs. (1) and (2) may lead to error accumulation of unacceptable magnitude during the course of the computation unless some correction scheme is used. One can iterate the solution many times, but we use the following approach, which is faster. Various compounds of a particular element are grouped into a hierarchy conserved within the family: for example, odd hydrogen, which is contained in H , OH , HO_2 , and H_2O_2 . The mass conservation equations for each

species are written, and then, after multiplying them by appropriate atom numbers, α_i , they are summed. The large values of P_i and $l_i n_i$, which merely account for shuffling of species within the family, cancel and we are left with

$$\begin{aligned} \partial S_H / \partial t &= -\partial \Phi_H / \partial z + \sum_H \alpha_i (P_i - l_i n_i) \\ &= -\partial \Phi_H / \partial z + P_T \end{aligned} \quad (5)$$

where $S_H = \sum_H \alpha_i n_i$ and Φ_H is the flux of odd hydrogen. For closed chemical systems $p_T = 0$, and for many systems of aeronomic interest, p_T will be a small residual net production or loss term that is much less than p_i and $l_i n_i$ of the individual species.

Table 3 Lower boundary conditions—O-H-N compounds

Constituent	Dominant boundary condition ^a	Flux value or equivalent ^b
$O(^3P)$	CE	0
$O(^1D)$	CE	0
O_3	Flux	$[O_3]_{10} = 3 \times 10^{11} \text{ cm}^{-3}$
NO	^d	^e
NO_2	^d	^e
OH	^d	$\Phi = -1 \times 10^5 \text{ cm}^{-2} \text{ sec}^{-1}$
H_2O	Flux	$[H_2O]_{10} = 3 \times 10^{13} \text{ cm}^{-3}$
H	CE	0
HO_2	^d	$\Phi = -1 \times 10^5 \text{ cm}^{-2} \text{ sec}^{-1}$
H_2O_2	^d	$\Phi = -4 \times 10^5 \text{ cm}^{-2} \text{ sec}^{-1}$
NO_3	CE	0
N_2O_5	CE	0
N_2O	Flux	$[N_2O]_{10} = 1.8 \times 10^{12} \text{ cm}^{-3}$
N	CE	0
HNO_3	Flux	^e
HNO_2	^d	^e
H_2	Flux	$[H_2]_{10} = 4 \times 10^{12} \text{ cm}^{-3}$

^a CE = chemical equilibrium.^b A positive value refers to an upward flux, a negative value to a downward flux.^c For certain long-lived species such as H_2O , O_3 , and N_2O , which are flux-controlled, the lower fluxes at 10 km were taken to be proportional to the difference between the computed density at the lower boundary and the density indicated in the table above, which is typical of measured values.^d These species are very close to chemical equilibrium at the lower boundary. The material flowing through the lower boundary rapidly approaches chemical equilibrium in the stratosphere.^e The total mixing ratio of odd nitrogen at the lower boundary is assumed to be near 5×10^{-10} by number. Upward or downward fluxes of the species NO, NO_2 , HNO_2 , and HNO_3 are used to achieve this boundary condition in the manner described in Footnote c above, where the total odd-N flux is divided among the species according to their densities.

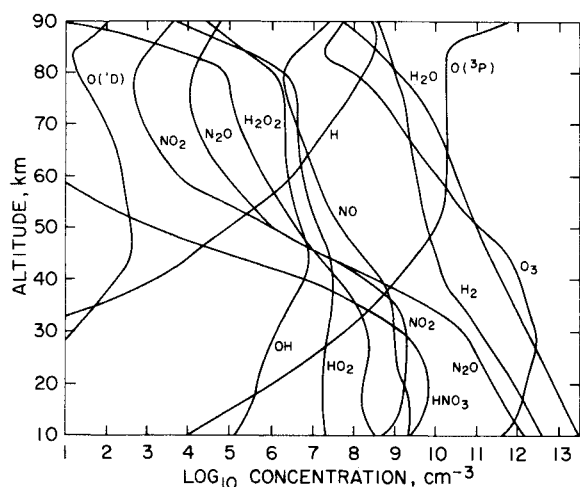


Fig. 2 Vertical distributions of various atmospheric constituents with eddy diffusion coefficient profile 1.

The value of S_H obtained by solving Eq. (5) is then compared with the sum

$$S = \sum_i \alpha_i n_i$$

obtained by computing the n_i of the individual species [Eqs. (1) and (2)]. The computed values of n_i can then be appropriately corrected, the simplest technique being to scale each of these by a factor of S_H/S . The results using this technique are comparable to those obtained by iterating 10 times at each time step. Moreover, near steady state, the solutions become highly accurate.

The choice of boundary conditions is crucial to the behavior of the vertical distributions of many of the constituents. In our work we do not impose strict flux or chemical equilibrium boundary conditions on our solutions. Instead, we have devised a technique in which a dummy level is established near the upper and lower boundaries, and both continuity and flux equations are used to start the solution at the bottom and to terminate it at the top (see Appendix A). If a species is dominated by chemistry, the corresponding terms will dominate the boundary condition and establish a value near the chemical equilibrium value. At the same time, the specified flux through the boundary can affect the over-all atom balance. Thus, the boundary fluxes for each constituent are still basic information for our model. At the upper boundary, zero fluxes were assumed except for NO and H; the former has a downward flux of $10^{12} \text{ cm}^{-2} \text{ sec}^{-1}$ and the latter, an upward flux equal to its escape rate ($10^7 \text{ cm}^{-2} \text{ sec}^{-1}$). The lower boundary condition for each constituent is specified in Table 3. In cases where a flux-dominated constituent (e.g., O_3 , H_2O) has been measured near the lower boundary, we set the boundary condition so that the measured value of the concentration is closely maintained during the computer run.

Ambient Atmosphere

Computed profiles of the minor constituents are shown in Figs. 2 and 3 for eddy profiles 1 and 2 which are shown in Fig. 1. The profiles of OH, O_3 , and $\text{O}(^1\text{D})$ agree reasonably well with observations of the first two,^{59,60} and with model predictions of all three.^{10,61-63} There is some disagreement, to be sure, such as the prediction of the ozone peak at about 28–30 km rather than the measured ~23–25 km, but they are minor. Overestimation of O_3 column density and prediction of the concentration peak at an altitude which is too high seems to be a feature of all one-dimensional models. In our model O_3 number density at 10 km is maintained near $3 \times 10^{11} \text{ cm}^{-3}$. The concentration of nitric oxide at high altitudes (60–90 km) as shown in Fig. 2 (low eddy diffusivity) seems to be too small when compared with measurements made from airglow observations.^{64,65}

The profile (Fig. 3) which corresponds to the high eddy diffusivity is in much better agreement with observed NO concentration, but the applicability of such large values of K_e is questionable. On the basis of one-dimensional models of atomic oxygen chemistry and transport, Colegrove et al.⁶⁶ estimated that K_e must be $\sim 5 \times 10^6 \text{ cm}^2 \text{ sec}^{-1}$ in the region just below the turbo-pause (~90–110 km). However, more recent work by Johnson and Gottlieb⁶⁷ who took into account meridional transport of atomic oxygen has lowered the estimate to $\sim 10^6 \text{ cm}^2 \text{ sec}^{-1}$. Moreover, Strobel⁶⁸ has questioned the reliability of the NO measurements. From model studies similar to ours he suggested mesospheric NO concentrations very close to those presented in Fig. 1.

The principal source of stratospheric NO_x in our model is reaction R28. A secondary source is production by galactic cosmic rays.⁶⁹ McConnell and McElroy⁷⁰ have also included the reaction $\text{OH} + \text{NH}_3 \rightarrow \text{H}_2\text{O} + \text{NH}_2$ as a source of NO_x ; the NH_2 is the first reaction in a chain which terminates in NO. However, as they point out, ammonia reactions can also lead to destruction of NO_x . Until the details of the ammonia chemistry are fully developed and the concentration of NH_3 in the lower stratosphere is determined, it seems to us to be somewhat idle to speculate further on the importance of atmospheric ammonia as a source of NO_x . Kaplan⁷¹ has recently placed an upper limit on the NH_3 mixing ratio in the upper troposphere and lower stratosphere of 0.08 ppb.

Measurements of nitrogen compounds at low altitudes have been carried out only recently. Using an infrared spectrometric technique, Murcray and co-workers⁷² have observed the nitric acid in the stratosphere to lie between 1 and $20 \times 10^9 \text{ cm}^{-3}$ with two rather sharp peaks occurring at 16 and 22 km. The HNO_3 profiles shown in Figs. 2 and 3 are of the same order of magnitude as the measurements, but the observed peaks are not present. At this point, we do not have any information about the origin of such structure. Nitric oxide and nitrogen dioxide have also been detected in the lower stratosphere. Schiff and co-workers⁷³ have observed NO, using the NO- O_3 chemiluminescent reaction, to have a concentration of about $3 \times 10^8 \text{ cm}^{-3}$ at 17 km altitude while Loewenstein⁷⁴ has observed values in the range 0.7 to $2 \times 10^8 \text{ cm}^{-3}$ at 21 km altitude. This value is to be compared with our prediction of $\sim 10^9 \text{ cm}^{-3}$. Investigations have also been carried out by Farmer and co-workers⁷⁵ and by Ackerman and co-workers.⁷⁶ The former obtained the very high value of about 10^{10} cm^{-3} of NO while the latter obtained 2 to $6 \times 10^8 \text{ cm}^{-3}$, which is much closer to the results of Schiff and Loewenstein.

The principal source of nitric acid in the stratosphere is the reaction of NO_2 with OH. In the upper stratosphere the reaction (R43) is a true three-body process, but at lower altitudes it is

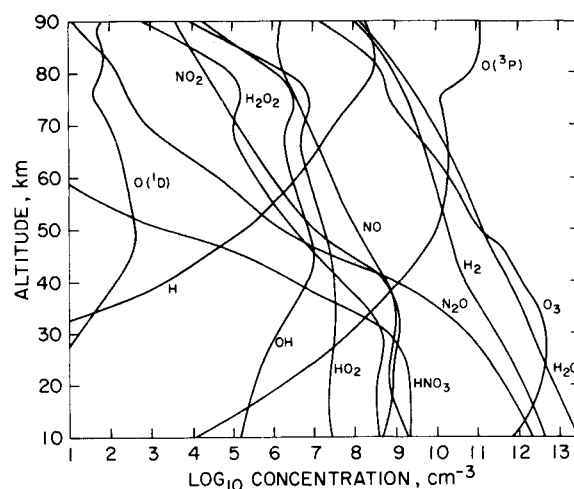


Fig. 3 Vertical distributions of various atmospheric constituents with eddy diffusion coefficient profile 2.

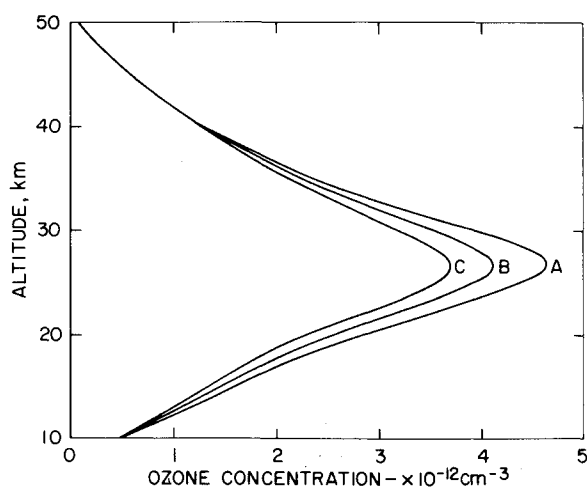


Fig. 4 Ozone profiles for various assumptions about deposition and meridional dispersion of SST exhaust: A, unperturbed atmosphere; B, deposition at 16 km altitude, dispersion over a zone 1000 km wide; C, deposition at 20 km altitude, dispersion over a zone 1000 km wide.

pressure-independent (effective two-body). This type of behavior reflects the formation of an unstable complex whose stabilization by collision is rapidly saturated as the number density of "third bodies" (i.e., the pressure) increases. There is still considerable uncertainty concerning the values of the various parameters which describe the stabilization process. The rate coefficient for reaction R43 needs to be more accurately determined.

There are also uncertainties in the choice of lower boundary conditions which may lead to erroneous values of the constituents at low altitudes. This is particularly true of ozone and odd nitrogen.

The ambient NO_x concentrations obtained in our model are somewhat lower than in that of McConnell and McElroy.⁷⁰ One reason for the difference probably lies in the rather different eddy diffusivity profiles employed in the two models. In the vicinity of 20 km altitude the McConnell-McElroy eddy diffusivity is nearly an order of magnitude less than the values given by profile 1 of Fig. 1. A second reason lies in the different lower boundary conditions used in the two models.

It is instructive, at this point, to look at the relative importance of nitric oxide and the water derivatives OH and HO_2 in reducing odd oxygen to even oxygen in the stratosphere.

In the lower stratosphere, reactions R13 and R26 are the most significant processes, the rate of destruction by NO_x being somewhat slower than the destruction by HO_x in our model. Thus, at 20 km altitude the rate of odd oxygen destruction due to R26 is $\sim 4 \times 10^4 \text{ cm}^{-3}\text{sec}^{-1}$, while that due to R13 is only $\sim 1.5 \times 10^4 \text{ cm}^{-3}\text{sec}^{-1}$. We therefore conclude that NO_x is of somewhat less importance than HO_x in reducing odd to even oxygen at 20 km. However, with ascending altitude NO_x becomes the more important. For example, at 30 km the rate of R13 is $1.5 \times 10^6 \text{ cm}^{-3}\text{sec}^{-1}$, whereas the rate of R26 is only $5 \times 10^5 \text{ cm}^{-3}\text{sec}^{-1}$. At 40 km the effect of NO_x relative to HO_x is even more pronounced.

Processes R10 and R12 also lead to reduction of oxygen, but their effective rates are limited by the rates of processes R26 and R13, respectively, since photolysis of HO_2 and especially NO_2 can regenerate oxygen atoms. Process R36 leads to a less important sink for odd oxygen through the photodissociation of NO_3 .

Perturbed Atmosphere

It is envisaged that by 1990 a very dense pattern of supersonic transport flight will exist over the North Atlantic Ocean, i.e., New York to London, Amsterdam, Frankfurt, and Paris. It is

estimated that with present-day engines, the daily effluent of NO_x in a box 500 km wide, 500 km long, and 2 km deep would be 28.7 metric tons⁷⁷; there are about 12 such boxes along the flight corridor. The corresponding water vapor daily effluent would be about 2000 metric tons.⁷⁸ One can simulate this perturbation by considering the emission to occur at a constant rate at 20 km altitude. We assume a steady nitric oxide emission rate of $6.6 \times 10^3 \text{ cm}^{-3}\text{sec}^{-1}$ (we consider all NO_x to be emitted as NO) and a water vapor emission rate of $4.8 \times 10^5 \text{ cm}^{-3}\text{sec}^{-1}$ in a box 1000 km wide, 6000 km long and 2 km deep. These data were fed into the program which was run for a period of two years. It was found that the water vapor deposition has no detectable effect on ozone balance, and only a very small effect on the water vapor distribution because of the large amount of the latter present in the ambient stratosphere. The nitric oxide emission does have an effect on the ozone distribution as well as on the NO, NO_2 , and HNO_3 distributions (Figs. 4 and 5). Curve A in Fig. 4 represents the ozone distribution in the ambient atmosphere, while curve C represents the SST-perturbed ozone layer; the latter corresponds to an ozone column density reduction of 15%. We also present ozone profile B, which corresponds to deposition at the original rate at 16 km rather than 20 km altitude. The reduction in ozone column density for profile B is 8%. Two features of these profiles are worthy of note: a) the greatest reduction in ozone concentration occurs at the concentration maxima, not at the deposition altitude; and b) if the altitude of deposition is lowered from 20 to 16 km, the ozone concentration is not affected as strongly as before. The latter effect is a pronounced one; it appears that aircraft which operate mainly at altitudes near 16 km will probably have a small effect on the ozone layer. The two effects (a) and (b) are related because they depend on vertical transport; the NO_x being transported upward from the aircraft deposition region.

Figure 5 demonstrates the importance of transport to the distributions of NO and HNO_3 ; although the deposition of NO from the SST fleet occurs at a single altitude (20 or 16 km), the odd nitrogen compounds spread vertically over a considerable range.

The reductions in ozone column density due to SST operations predicted by our model are in rather sharp disagreement with those suggested by Johnston⁷⁹ and Stewart and Hoffert,⁸⁰ who obtained reductions of as much as 50% and 70%, respectively. Crutzen^{81,82} indicates that his estimates of reduction in ozone column densities are of the same order as ours. Johnston did not take account of transport, nor did he realize the importance of HNO_3 as a reservoir for odd nitrogen. We do not know the reason for Stewart's large estimates. One of the factors underlying

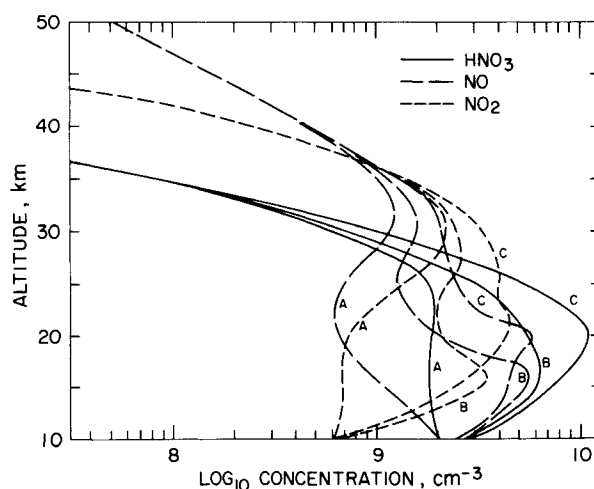


Fig. 5 Vertical distributions of odd nitrogen compounds NO, NO_2 , and HNO_3 . For definition of curve labels (A-C) refer to Fig. 4.

the small decrease in ozone is a "self-healing" effect which acts to restore the ozone after it is destroyed. Reduction of the ozone column density results in an increase in the rate of photo-dissociation of O_2 (process J2) in the stratosphere. The atomic oxygen so released reacts with O_2 to reform ozone (reaction R1).

Next, consider the space shuttle vehicle. During the entry phase, this vehicle forms about 2–8 metric tons of NO with a quite uniform vertical distribution between 70 and 90 km.⁸³ It is anticipated that there will be both low inclination and polar orbits, but in the following discussion of environmental effects we assume all orbits to be polar. A schematic diagram of the entry trajectory is shown in Fig. 6; we have divided the trajectory into segments, each 10° of latitude wide. In each segment we assume that the NO formed during entry is uniformly mixed throughout a box 10° of latitude wide, 4 km deep (centered in altitude at the passage of the trajectory through the midpoint of the segment), and $2\pi R_e \cos \lambda_m$ km long. Here, R_e is the radius of the Earth and λ_m is the latitude of the midpoint of the segment. In other words, the NO is assumed to be completely dispersed by winds and eddies over a zone. Our study assumes fifty entries per year; hence we have injected a pulse of NO into each box every 6×10^5 sec, and allowed the program to run for 3×10^7 sec simulated time. The results are shown in Fig. 7. There is a small effect on NO but not on the distribution of other nitrogen compounds nor on the ozone profile.

Conclusions

It is apparent that predicted space shuttle re-entries are not likely to have a significant effect on the NO_x and O_3 balances in the stratosphere and mesosphere; the predicted effect of SST operations is not large. A substantial improvement in the NO_x emission characteristics of jet engines, which is quite possible by 1990, would reduce the effect even further. However, the one-dimensional model described here is limited because it cannot quantitatively take account of horizontal spreading of the artificially produced NO_x , nor can it take complete account of the entry trajectory of the space shuttle vehicle which slants through the mesosphere for many thousands of kilometers. In the studies reported here, we have used daytime steady-state conditions only. The model should be run with diurnal variation to evaluate fully the effects of NO_x ; we hope to perform these computations soon. To attack the problem of NO_x realistically, one must use at least a two-dimensional zonal model. Such a model is being developed at Ames, as well as by Shimazaki,⁸⁴ but we do not yet have results from it.

Appendix A: Finite-Difference Equations at the Lower Boundary

The continuity equation for a species at the lower boundary in finite difference form can be written

$$A_0 N_2 + B_0 N_1 + C_0 N_0 = D_0 \quad (A1)$$

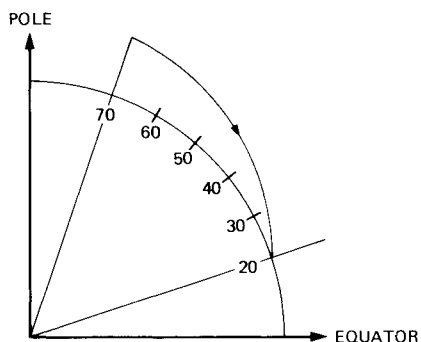


Fig. 6 Entry trajectory of space shuttle vehicle from polar orbit; vertical scale is exaggerated.

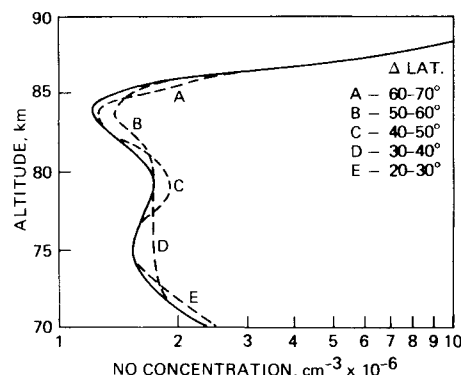


Fig. 7 Mesospheric nitric oxide concentration profiles. The broken lines refer to perturbations caused by space shuttle vehicle entry for one year of operations with 50 entries.

where N_k is the species density at altitude level k , and A , B , C , and D are coefficients which are functions of known quantities at the lower boundary. Level 0 is a "dummy" level below the lower boundary, level 1.

The corresponding flux equation at the lower boundary for our model can be written as

$$\Phi \equiv \Phi_B + V_B(N_B - N_1) = E(N_2 - N_0) + FN_1 \quad (A2)$$

Here E and F are known coefficients. The boundary flux is expressed by two terms, but only one of these is generally used for any species. Φ_B represents a fixed boundary flux which may be specified when appropriate. The second term, on the other hand, gives a flux in terms of the difference between a fixed boundary density N_B and the instantaneous density at the boundary, N_1 . The velocity V_B represents the coupling across the boundary layer in a very simplified way. Nominally, we choose $V_B = 1$ cm sec⁻¹. Such a flexible boundary specification should be more realistic than rigidly fixing the boundary density.

Equations (A1) and (A2) are now combined to obtain one equation between N_1 and N_2 which can then be compared to the "marching" equation which propagates the solution (e.g., Shimazaki⁵⁸)

$$N_1 = K_1 - L_1 N_2 \quad (A3)$$

to obtain the coefficients K_1 and L_1 which start the solution at the lower boundary. A similar procedure at the upper boundary terminates the computational sequence which fix the K and L coefficients.

Our model also has the capability for studying the effects of vertical convection on minor species distributions. However, recognizing that vertical convection is associated with horizontal velocity gradients we have devised a simple convection model which also accounts approximately for the horizontal divergence. We first note that the divergence of the molecular flux in a steady state atmosphere is zero, or

$$\nabla \cdot (N_M \mathbf{V}) = 0 \quad (A4)$$

where N_M is the total atmospheric density. For any minor species N the flux divergence due to convection may be put in the form

$$\nabla \cdot \Phi_{\text{conv}} = \nabla \cdot (N\mathbf{V}) = N_M \mathbf{V} \cdot \nabla (N/N_M) \quad (A5)$$

Now, if we assume that horizontal gradients in N/N_M are negligible, we have conveniently

$$\nabla \cdot \Phi_{\text{conv}} = N_M V_z (\partial/\partial z) (N/N_M) \quad (A6)$$

for our one-dimensional model.

References

- Strobel, D. F., "Diurnal Variation of Nitric Oxide in the Upper Atmosphere," *Journal of Geophysical Research*, Vol. 76, No. 10, April 1971, pp. 2441–2452.
- Hays, P. B. and Oliveira, J. J., "Carbon Dioxide and Monoxide Above the Tropopause," *Planetary and Space Science*, Vol. 18, No. 12, Dec. 1970, pp. 1729–1734.

- ³ Zimmerman, S. P., private communication, 1972, Air Force Cambridge Research Labs., Bedford, Mass.
- ⁴ Huie, R. E., Herron, J. T., and Davis, D. D., "Absolute Rate Constants for the Reaction $O + O_2 + M \rightarrow O_3 + M$ Over the Temperature Range 200–364°K," *Journal of Physical Chemistry*, Vol. 76, No. 19, Sept. 1972, pp. 2653–2658.
- ⁵ Campbell, I. M. and Thrush, B. A., "The Association of Oxygen Atoms and Their Combination With Nitrogen Atoms," *Proceedings of the Royal Society, London, Ser. A*, Vol. 296, No. 1445, Jan. 1967, pp. 222–232.
- ⁶ Johnston, H. S., "Gas Phase Reaction Kinetics of Neutral Oxygen Species," *National Standard Reference Data Series NBS-20*, U.S. Government Printing Office, Washington, D.C., Sept. 1968, pp. 21–34.
- ⁷ Gilpin, R., Schiff, H. I., and Welge, K. H., "Photodissociation of O_3 in the Hartley Band; Reactions of $O(^1D)$ and $O_2(^1\Sigma^+)$ with O_3 and O ," *Journal of Chemical Physics*, Vol. 55, No. 3, Aug. 1971, pp. 1087–1093.
- ⁸ Noxon, J. F., "Optical Emission from $O(^1D)$ and $O_2(b^1\Sigma^+)$ in the Ultraviolet Photolysis of O_2 and CO_2 ," *Journal of Chemical Physics*, Vol. 52, No. 4, Feb. 1970, pp. 1852–1873.
- ⁹ Baulch, D. L., Drysdale, D. D., Horne, D. G., and Lloyd, A. C., *Evaluated Kinetic Data for High Temperature Reactions*, Vol. 1, CRC Press, Cleveland, Ohio, 1972, pp. 37, 157, 193, 261.
- ¹⁰ Nicolet, M., "Aerochemistry of the Stratosphere," *Planetary and Space Science*, Vol. 20, No. 10, Oct. 1972, pp. 1671–1702.
- ¹¹ Kaufman, F., "Neutral Reactions," *DASA Reaction Rate Handbook*, edited by M. H. Bortner, DASA 1948, General Electric Co., Santa Barbara, Calif., 1967, p. 14–1.
- ¹² Anderson, J. G. and Kaufman, F., "Kinetics of the Reaction $OH + NO_2 + M \rightarrow HNO_3 + M$," *Chemical Physics Letters*, Vol. 16, No. 2, Oct. 1972, pp. 375–379.
- ¹³ Kurylo, M. J., "Absolute Rate Constants for the Reaction $H + O_2 + M \rightarrow HO_2 + M$ Over the Temperature Range 203–404 K," *Journal of Physical Chemistry*, Vol. 76, No. 24, Nov. 1972, pp. 3518–3526.
- ¹⁴ Davis, D. D., Herron, J. T., and Huie, R. E., "Absolute Rate Constants for the Reaction $O(^3P) + NO_2 \rightarrow NO + O_2$ Over the Temperature Range 339–230 K," *Journal of Chemical Physics*, Vol. 58, No. 2, Jan. 1973, pp. 530–535.
- ¹⁵ Baulch, D. L., Drysdale, D. D., and Horne, D. G., "Critical Evaluation of Rate Data for Homogeneous Gas Phase Reactions of Interest in High Temperature Systems," *High Temperature Reaction Rate Data Rept. 5*, Univ. of Leeds, Leeds, England, July 1970, pp. 15–23.
- ¹⁶ Hochanadel, C. J. and Ghormley, J. A., "Absorption Spectrum and Reaction Kinetics of the HO_2 Radical in the Gas Phase," *Journal of Chemical Physics*, Vol. 56, No. 9, May 1972, pp. 4426–4432.
- ¹⁷ Kondratiev, V. N., *Rate Constants of Gas Phase Reactions*, Izdatel'stvo "Nauka," Moskva, 1970, edited by R. M. Fristrom (Translated from the Russian), National Tech. Info. Service COM-72-10014, Jan. 1972, p. 13.
- ¹⁸ Lloyd, A. C., "Evaluated and Estimated Kinetic Data for the Gas Phase Reactions of Hydroperoxyl Radical," Rept. 10447, 1970, National Bureau of Standards, Washington, D.C.
- ¹⁹ Nicolet, M., "Aeronomical Reactions of Hydrogen and Ozone," in *Mesospheric Models and Related Experiments*, edited by G. Fiocco, D. Reidel Publishing Co., Dordrecht-Holland, 1971, pp. 1–51.
- ²⁰ Young, R. A., Black, G., and Slinger, T. G., "Reaction and Deactivation of $O(^1D)$," *Journal of Chemical Physics*, Vol. 49, No. 11, Dec. 1968, pp. 4758–4776.
- ²¹ Wilson, W. E., "A Critical Review of the Gas-Phase Reaction Kinetics of the Hydroxyl Radical," *Journal of Physical Chemistry, Ref. Data*, Vol. 1, No. 2, 1972, pp. 535–573.
- ²² Simonaitis, R., Greenberg, R. I., and Heicklen, J., "Photolysis of N_2O at 2139 Å and 1949 Å," *International Journal of Chemical Kinetics*, Vol. 4, No. 5, Sept. 1972, pp. 497–512.
- ²³ Wilson, W. E., "Rate Constant for the Reaction $N + O_2 \rightarrow NO + O$," *Journal of Chemical Physics*, Vol. 46, No. 5, March 1967, pp. 2017–2018.
- ²⁴ Phillips, L. F. and Schiff, H. I., "Mass Spectrometric Studies of Atomic Reactions V., Reaction of Nitrogen Atoms with NO ," *Journal of Chemical Physics*, Vol. 42, No. 9, May 1965, pp. 3171–3174.
- ²⁵ Ford, H. W. and Jaffe, S., "Photolysis of Nitrogen Dioxide at 3660 and 4047 Å at 25°C," *Journal of Chemical Physics*, Vol. 38, No. 12, June 1963, pp. 2935–2942.
- ²⁶ Bahn, G. S., "Chemical Kinetics," *Pyrodynamics*, Vol. 1, 1964, pp. 147, 271, 335; Vol. 2, 1965, pp. 91, 197, 315; Vol. 3, 1965, p. 245; Vol. 6, 1968, p. 110.
- ²⁷ Davis, D. D., Wong, W. W., Fischer, S. D., Schiff, R. L., Lephardt, J. O., Prusaczyk, J. E., Payne, W. A., Stief, L. J., Huie, R. E., and Herron, J. T., "Recent Kinetic Measurements on the Reactions of $O(^3P)$, H, and HO_2 ," *Proceedings of the Second Conference on the Climatic Impact Assessment Program*, Nov. 14–17, 1972; Rept. DOT-TSC-OST-73-4, 1973, U.S. Dept. of Transportation, Washington, D.C., pp. 126–143.
- ²⁸ Westenberg, A. A. and deHaas, N., "Rate Measurements on $OH + NO + M$ and $OH + NO_2 + M$," *Journal of Chemical Physics*, Vol. 57, No. 12, Dec. 1972, pp. 5375–5378.
- ²⁹ Bascombe, K. N., "Reaction Rate Data: The Hydrogen/Oxygen System," E.R.D.E. Rept. 1/5/65, 1965, Ministry of Aviation, Waltham Abbey, U.K.
- ³⁰ Peterson, H. L. and Kretschmer, C. B., "Kinetics of Recombination of Atomic Oxygen at Room Temperatures," Rept. OTS, 1960, U.S. Dept. of Commerce, Washington, D.C.
- ³¹ Phillips, L. F. and Schiff, H. I., "Mass Spectrometric Studies of Atom Reactions, I. Reactions in the Atomic Nitrogen-Ozone System," *Journal of Chemical Physics*, Vol. 36, No. 6, March 1962, pp. 1509–1517.
- ³² Klein, F. S. and Herron, J. T., "Mass Spectrometric Study of the Reactions of O Atoms with NO and NO_2 ," *Journal of Chemical Physics*, Vol. 41, No. 5, Sept. 1965, pp. 1285–1290; "Erratum," *Journal of Chemical Physics*, Vol. 44, No. 9, May 1965, pp. 3645–3646.
- ³³ Johnston, H. S., "Four Mechanisms Involving Nitrogen Pentoxide," *Journal of the American Chemical Society*, Vol. 73, 1951, pp. 4542–4546.
- ³⁴ Simonaitis, R., Lissi, E., and Heicklen, J., "On the Production of N_2O From the Reaction of $O(^1D)$ with N_2 ," *Journal of Geophysical Research*, Vol. 77, No. 22, Aug. 1972, pp. 4248–4250.
- ³⁵ Hudson, R. D. and Mahle, S. H., "Photodissociation Rates of Molecular Oxygen in the Mesosphere and Lower Thermosphere," *Journal of Geophysical Research*, Vol. 77, No. 16, June 1972, pp. 2902–2914.
- ³⁶ Ogawa, M., "Absorption Coefficients of O_2 at the Lyman-Alpha Line and its Vicinity," *Journal of Geophysical Research*, Vol. 73, No. 21, Nov. 1968, pp. 6759–6763.
- ³⁷ Blake, A. J., Carver, J. H., and Haddad, G. N., "Photoabsorption Cross Section of Molecular Oxygen Between 1250 Å and 2350 Å," *Journal of Quantitative Spectroscopy and Radiative Transfer*, Vol. 6, No. 4, July/Aug. 1966, pp. 451–459.
- ³⁸ Watanabe, K., Inn, E. C. Y., and Zelikoff, M., "Absorption Coefficients of Oxygen in the Vacuum Ultraviolet," *Journal of Chemical Physics*, Vol. 21, No. 6, June 1953, pp. 1026–1030.
- ³⁹ Inn, E. C. Y. and Tanaka, Y., "Absorption Coefficient of Ozone in the Ultraviolet and Visible Regions," *Journal of the Optical Society of America*, Vol. 43, No. 10, Oct. 1953, pp. 870–873.
- ⁴⁰ Griggs, M., "Absorption Coefficients of Ozone in the Ultraviolet and Visible Regions," *Journal of Chemical Physics*, Vol. 49, No. 2, July 1968, pp. 857–859.
- ⁴¹ Jones, I. T. N. and Wayne, R. P., "Photolysis of Ozone by 254-, 313-, and 334-nm Radiation," *Journal of Chemical Physics*, Vol. 51, No. 8, Oct. 1969, pp. 3617–3618.
- ⁴² Hall, T. C. and Blacet, F. E., "Separation of the Absorption Spectra of NO_2 and N_2O_4 in the Range 2460–5000 Å," *Journal of Chemical Physics*, Vol. 20, No. 11, Nov. 1952, pp. 1745–1749.
- ⁴³ Nakayama, T., Kitamura, M. Y., and Watanabe, K., "Ionization Potential and Absorption Coefficients of Nitrogen Dioxide," *Journal of Chemical Physics*, Vol. 30, No. 5, May 1959, pp. 1180–1186.
- ⁴⁴ Pitts, J. N., Sharp, J. H., and Chan, S. I., "Effects of Wavelength and Temperature on Primary Processes in the Photolysis of Nitrogen Dioxide and a Spectroscopic-Photochemical Determination of the Photodissociation Energy," *Journal of Chemical Physics*, Vol. 40, No. 12, June 1964, pp. 3655–3662.
- ⁴⁵ Zelikoff, M., Watanabe, K., and Inn, E. C. Y., "Absorption Coefficients of Gases in the Vacuum Ultraviolet, II. Nitrous Oxide," *Journal of Chemical Physics*, Vol. 21, No. 10, Oct. 1953, pp. 1643–1647.
- ⁴⁶ Bates, D. R. and Hays, P. B., "Atmospheric Nitrous Oxide," *Planetary and Space Science*, Vol. 15, No. 1, Jan. 1967, pp. 189–198.
- ⁴⁷ Preston, K. F. and Barr, R. F., "Primary Processes in the Photolysis of Nitrogen Dioxide," *Journal of Chemical Physics*, Vol. 54, No. 8, April 1971, pp. 3347–3348.
- ⁴⁸ Jones, E. J. and Wulf, O. R., "The Absorption Coefficient of Nitrogen Pentoxide in the Ultraviolet and the Visible Absorption Spectrum of NO_3 ," *Journal of Chemical Physics*, Vol. 5, No. 11, Nov. 1937, pp. 873–877.
- ⁴⁹ Johnston, H. S. and Graham, R., "Gas-Phase Ultraviolet Absorption Spectrum of Nitric Acid Vapor," *Journal of Physical Chemistry*, Vol. 77, No. 1, Jan. 1972, pp. 62–63.
- ⁵⁰ Johnston, H. S., *CIAP Newsletter 72-4*, U.S. Dept. of Transportation, Washington, D.C., December 8, 1972, p. 1.

- ⁵¹ Watanabe, K. and Zelickoff, M., "Absorption Coefficients of Water Vapor in the Ultraviolet," *Journal of the Optical Society of America*, Vol. 43, No. 9, Sept. 1953, pp. 753-755.
- ⁵² Urey, H. C., Dawsey, L. H., and Rice, F. O., "The Absorption Spectrum and Decomposition of Hydrogen Peroxide by Light," *Journal of American Chemical Society*, Vol. 51, 1929, p. 1371.
- ⁵³ Hold, R. B., McLane, C. K., and Oldenberg, O., "Ultraviolet Absorption Spectrum of Hydrogen Peroxide," *Journal of Chemical Physics*, Vol. 16, No. 3, March 1948, pp. 225-229.
- ⁵⁴ Paukert, T. T. and Johnston, H. S., "Spectra and Kinetics of the Hydroperoxyl Free Radical in the Gas Phase," *Journal of Chemical Physics*, Vol. 56, No. 6, March 1973, pp. 2824-2838.
- ⁵⁵ Johnston, H. S., "Project Clean Air," Task Force No. 7, Univ. of California, Berkeley, 1970.
- ⁵⁶ Detwiler, C. R., Garrett, D. L., Purcell, J. D., and Towsey, R., "The Intensity Distribution in the Ultraviolet Solar Spectrum," *Annales de Géophysique*, Vol. 17, No. 3, July-Sept. 1961, pp. 263-272.
- ⁵⁷ Parkinson, W. H. and Reeves, E. M., "Measurements in the Solar Spectrum Between 1400 and 1875 Å with a Rocket-Borne Spectrometer," *Solar Physics*, Vol. 10, No. 2, Dec. 1969, pp. 342-347.
- ⁵⁸ Shimazaki, T., "Dynamic Effects on Atomic and Molecular Oxygen Density: A Numerical Solution to Equations of Motion and Continuity," *Journal of Atmospheric and Terrestrial Physics*, Vol. 29, No. 6, June 1967, pp. 723-748.
- ⁵⁹ Anderson, J. G., "Rocket-Borne Ultraviolet Spectrometer Measurements of OH Resonance Fluorescence with a Diffusive Transport Model for Mesospheric Photochemistry," *Journal of Geophysical Research*, Vol. 76, No. 19, July 1971, pp. 4634-4652.
- ⁶⁰ Dutsch, H. U., "Photochemistry of Atmospheric Ozone," *Advances in Geophysics*, Vol. 15, Academic Press, New York, 1971, pp. 219-322.
- ⁶¹ Shimazaki, T. and Laird, A. R., "Seasonal Effects on Distributions of Minor Neutral Constituents in the Mesosphere and Lower Thermosphere," *Radio Science*, Vol. 7, No. 1, Jan. 1972, pp. 23-43.
- ⁶² Wofsy, S. C., McConnell, J. C., and McElroy, M. B., "Atmospheric CH₄, CO, and CO₂," *Journal of Geophysical Research*, Vol. 77, No. 24, Aug. 1972, pp. 4477-4493.
- ⁶³ Brasseur, G. and Nicolet, M., "Chemospheric Processes of Nitric Oxide in the Mesosphere and Stratosphere," *Planetary and Space Science*, Vol. 21, No. 6, June 1973, pp. 939-962.
- ⁶⁴ Meira, L. G., "Rocket Measurements of Upper Atmospheric Nitric Oxide and Their Consequences to the Lower Ionosphere," *Journal of Geophysical Research*, Vol. 76, No. 1, Jan. 1971, pp. 202-212.
- ⁶⁵ Tisone, G. C., "Measurements of NO Densities During Sunrise at Kauai," *Journal of Geophysical Research*, Vol. 78, No. 4, Feb. 1973, pp. 746-750.
- ⁶⁶ Colegrove, F. D., Hanson, W. B., and Johnson, F. S., "Eddy Diffusion and Oxygen Transport in the Lower Thermosphere," *Journal of Geophysical Research*, Vol. 70, No. 19, Oct. 1965, pp. 4931-4942.
- ⁶⁷ Johnson, F. S. and Gottlieb, B., "Atomic Oxygen Transport in the Thermosphere," *Planetary and Space Science*, Vol. 21, No. 6, June 1973, pp. 1001-1010.
- ⁶⁸ Strobel, D. F., "Nitric Oxide in the D-Region," *Journal of Geophysical Research*, Vol. 77, No. 7, March 1972, pp. 1337-1339.
- ⁶⁹ Warneck, P., "Cosmic Radiation as a Source of Odd Nitrogen in the Stratosphere," *Journal of Geophysical Research*, Vol. 77, No. 33, Nov. 1972, pp. 6589-6591.
- ⁷⁰ McConnell, J. C. and McElroy, M. B., "Odd Nitrogen in the Atmosphere," *Journal of the Atmospheric Sciences*, Vol. 30, No. 8, Nov. 1973, pp. 1465-1480.
- ⁷¹ Kaplan, L. D., "Background Concentrations of Photochemically Active Trace Constituents in the Stratosphere and Upper Troposphere," *Pure and Applied Geophysics*, Vols. 106-108, Nos. V-VII, 1973, pp. 1341-1345.
- ⁷² Williams, W. J., Brooks, J. N., Murcray, D. G., Murcray, F. H., Fried, P. M., and Weinman, J. A., "Distribution of Nitric Acid Vapor in the Stratosphere as Determined from Infrared Atmospheric Emission Data," *Journal of the Atmospheric Sciences*, Vol. 29, No. 7, Oct. 1972, pp. 1375-1379.
- ⁷³ Ridley, B. A., Schiff, H. I., Shaw, A. W., Bates, L., Howlett, C., LeVaux, H., McGill, L. R., and Ashenfelder, T. E., "Measurements in situ of Nitric Oxide in the Stratosphere between 17.4 and 22.9 km," *Nature*, Vol. 245, No. 5424, Oct. 1973, pp. 310-311.
- ⁷⁴ Loewenstein, M., private communication, 1974, NASA Ames Research Center, Moffett Field, Calif.
- ⁷⁵ Toth, R. A., Farmer, C. B., Schindler, R. A., Raper, O. F., and Schaper, P. W., "Detection of Nitric Oxide in the Lower Stratosphere," *Nature Physical Science*, Vol. 244, No. 131, July 1973, pp. 7-8.
- ⁷⁶ Ackerman, M., Frimout, D., Muller, C., Nevejans, D., Fontanella, J.-C., Girard, A., and Louisnard, N., "Stratospheric Nitric Oxide from Infrared Spectra," *Nature*, Vol. 245, No. 5422, Sept. 1973, pp. 205-206.
- ⁷⁷ CIAP Monograph 2, Climatic Impact Assessment Program, U.S. Dept. of Transportation, to be published, 1975.
- ⁷⁸ Broderick, A. J., English, J. M., and Forney, A. K., "An Initial Estimate of Aircraft Emissions in the Stratosphere in 1990," AIAA Paper 73-508, Denver, Colo., 1973.
- ⁷⁹ Johnston, H. S., "Reduction of Stratospheric Ozone by Nitrogen Oxide Catalysts from Supersonic Transport Exhaust," *Science*, Vol. 173, Aug. 6, 1971, pp. 517-522.
- ⁸⁰ Stewart, R. W. and Hoffert, M. I., "Stratospheric Contamination Experiments with a One-Dimensional Atmospheric Model," AIAA Paper 73-531, Denver, Colo., 1973.
- ⁸¹ Crutzen, P. J., "Ozone Production Rates in an Oxygen-Hydrogen-Nitrogen Oxide Atmosphere," *Journal of Geophysical Research*, Vol. 76, No. 30, Oct. 1971, pp. 7311-7327.
- ⁸² Crutzen, P. J., "SST's—A Threat to the Earth's Ozone Shield," *AMBIO*, Vol. 1, No. 2, April 1972, pp. 41-51.
- ⁸³ Park, C., "Estimates of Nitric Oxide Production for Lifting Spacecraft Reentry," TM X-62052, Aug. 1972, NASA.
- ⁸⁴ Shimazaki, T., Wuebbles, D. J., and Ogawa, T., "A Theoretical Model for Stratospheric Ozone Density Distributions in the Meridional Plane," AIAA Paper 73-541, Denver, Colo., 1973.